Lipids in Health and Disease

RESEARCH

Open Access

Resveratrol improved atherosclerosis by increasing LDLR levels via the EGFR-ERK1/2 signaling pathway

Dandan Hu[1,2†], Litian Wang[3†], Lin Qi[1,2†], Xiangxuan Yang[1,4], Yamin Jin[1,4], Huailiu Yin[1,4], Yewei Huang[1,2*], Jun Sheng[1*] and Xuanjun Wang[1,5*]

Abstract

Background and aims Atherosclerosis (AS) is a complex and chronic vascular disease and elevated low-density lipoprotein cholesterol (LDL-C) level is one of its primary causative factors. As a key surface receptor, low-density lipoprotein receptor (LDLR) plays an essential role in LDL-C clearance. Resveratrol (RSV) has emerged as a promising compound for investigating potential therapeutic targets for AS due to its ability to lower cholesterol, reduce endothelial anti-inflammatory and suppress vascular smooth muscle cell proliferation. This study explored the effects of RSV on AS through upregulating LDLR and analyzed the mechanism through a combination of in *vivo* and *vitro* experiments.

Methods HepG2 cells were exposed to varying concentrations of RSV. The effects of RSV on LDLR expression and cholesterol uptake were analyzed by western blot, RT-qPCR and DiI-LDL uptake assay. In *vivo*, C57BL/6J ApoE$^{-/-}$ mice were used and the experimental groups were treated with RSV, Lovastatin and Gefitinib. Plaque formation in the arteries and aortic roots was assessed by Oil Red O staining and plaque stability was evaluated using Hematoxylin-Eosin (H&E) and Elastic Van Gieson (EVG) staining. Western blot, RT-qPCR and immunohistochemical staining were employed to analyze the expression of LDLR in the livers of mice.

Results RSV significantly enhanced the stability of LDLR mRNA and promoted LDLR protein expression. The inhibition experiments of EGFR signaling pathway (Cetuximab and Gefitinib) demonstrated that the efficacy of RSV was markedly weakened when this signaling pathway was inhibited. It indicated that RSV modulated LDLR gene expression by activating EGFR-ERK1/2 pathway. In ApoE$^{-/-}$ mice, RSV notably reduced arterial plaque formation, improved plaque stability and increased hepatic LDLR expression.

†Dandan Hu, Litian Wang and Lin Qi contributed equally to this work.

*Correspondence:
Yewei Huang
lichuangyewei100@163.com
Jun Sheng
shengj@ynau.edu.cn
Xuanjun Wang
jwang@ynau.edu.cn

Full list of author information is available at the end of the article

Conclusion This study elucidated the mechanism by which RSV upregulates LDLR gene expression through activating EGFR-ERK1/2 signaling pathway. In *vivo* experiments demonstrated its efficacy in reducing arterial plaque formation and stabilizing existing plaques. These results further indicated that RSV held potential therapeutic value for ameliorating atherosclerosis and cardiovascular diseases. Collectively, these findings provided novel theoretical support for RSV's potential role in cardiovascular therapy.

Keywords Resveratrol (RSV), Low-density lipoprotein receptor (LDLR), Cardiovascular diseases, Atherosclerosis (AS), Cholesterol metabolism

Introduction

Atherosclerosis (AS) is a progressive and long-term disease widely recognized as a critical pathogenic factor for severe diseases, including acute coronary syndrome, cerebral ischemia and peripheral vascular diseases. AS exhibits high global morbidity and mortality rates, posing a significant threat to human life and health [1, 2]. Consequently, effective prevention and treatment strategies for AS have garnered considerable attention within the global medical community. Research indicates that the etiology of atherosclerosis is closely associated with the deposition of low-density lipoprotein cholesterol (LDL-C) [3]. As a key component of cholesterol, LDL-C can penetrate the vascular endothelium, accumulate in the vascular wall and form atherosclerotic plaques [4, 5]. Therefore, controlling LDL-C level is considered a crucial strategy for preventing and treating AS.

Low-density lipoprotein receptor (LDLR), widely distributed on extrahepatic cell membranes, is a key molecule in regulating plasma LDL-C [6, 7]. Statistically, approximately 75% of plasma LDL-C is degraded through the LDLR pathway, which indicates the pivotal role of LDLR in the clearance of endogenous cholesterol [8]. Due to its essential function in LDL cholesterol removal, LDLR is considered a highly promising target for anti-atherosclerotic therapy.

Mechanistically, LDLR expression exhibits high regulatory complexity and post-transcriptional regulation plays a particularly critical role. LDLR mRNA is an unstable transcript containing multiple cis-regulatory elements embedded in its 3' untranslated region (3'UTR), which form complexes with trans-regulatory RNA-binding proteins to regulate the stability and degradation rate of LDLR mRNA [9, 10]. Recent studies have demonstrated that ERK is a key mechanism regulating LDLR gene expression. Specifically, ERK activation stabilizes LDLR mRNA and enhances its expression level [11]. For instance, trixirabine has been shown to stabilize LDLR mRNA and augment cellular LDL uptake via an ERK-dependent mechanism [12], while caffeine promotes LDLR expression through EGFR-ERK1/2 pathway [13]. In summary, ERK signaling pathway is crucial for maintaining LDLR mRNA stability and regulating LDL-C clearance.

As a polyphenolic compound naturally present in various fruits and foods, Resveratrol (RSV) has received notable attention in recent years. RSV exhibits a wide range of biological effects, including antioxidant, anti-inflammatory, anti-aging and cardioprotective properties [14, 15]. Its antioxidant properties can mitigate cellular damage and delay aging by neutralizing free radicals [16]. The anti-inflammatory effect helps to lower the risk of related diseases through its anti-inflammatory action [17, 18]. In terms of cardiovascular protection, RSV can lower cholesterol levels and slow the progression of AS [19, 20]. Specifically, studies have demonstrated that RSV can significantly improve arterial function by inhibiting atherosclerotic plaque formation and reducing cholesterol accumulation in macrophages through activating PPARα/γ signaling pathway [21]. Additionally, administering RSV in patients with metabolic diseases effectively diminishes foam cell formation, improves endothelial dysfunction and reduces total cholesterol content [22, 23]. However, research on the role of RSV in slowing AS development by upregulating LDLR expression remains limited. This study aims to investigate whether RSV can alleviate AS progression by regulating LDLR expression and elucidate the underlying molecular mechanisms.

In this study, it was found that RSV enhanced the stability of LDLR mRNA by activating EGFR-ERK1/2 signaling pathway and eventually upregulated the expression level of LDLR. This molecular mechanism is expected to explain the protective effect of RSV in anti-atherosclerosis and offer a crucial theoretical basis for developing novel RSV-based therapeutic approaches for cardiovascular diseases. This finding not only expands the understanding of the pharmacological mechanism of RSV, but also provides a theoretical foundation for cardiovascular disease therapies.

Materials and methods

Reagents

RSV (purity > 98%), Cetuximab, Lovastatin and Gefitinib were obtained from Shanghai Yuanye Biotech. Co. Ltd. (Shanghai, China). Anti-LDLR, β-actin and β-tubulin antibodies were sourced from Cell Signaling Technology (Boston, USA). Anti-EGFR, P-EGFR, ERK and P-ERK antibodies were purchased from Abclonal Technology Co., Ltd. (Wuhan, China). Improved Oil Red O Staining

Kit, Collagen Fiber and Elastic Fiber Staining Kit and Hematoxylin-Eosin (H&E) Stain Kit were sourced from Solarbio Science and Tech. Co., Ltd. (Beijing, China). Total cholesterol (TC), triglyceride (TG), LDL-C and high-density lipoprotein cholesterol (HDL-C) assay kits were purchased from Nanjing Jiancheng Bioengineering Institute (Nanjing, China).

Cell culture

HepG2 cells (ATCC, Manassas, VA, USA) were cultured in DMEM medium supplemented with 10% fetal bovine serum (FBS) and 1% penicillin-streptomycin antibiotics (Solarbio, Beijing, China). Cells were thawed in 37.5°C water bath and transferred to a 15 mL centrifuge tube. Then, HepG2 cells were resuspended in fresh medium and seeded into 100 mm dishes. Cells were incubated at 37.5°C in an incubator containing 5% carbon dioxide.

Cell viability assay

HepG2 cells were seeded in 96-well plates. Cells were treated with RSV (0–60 μM) for 24 h. Subsequently, cells were incubated with 5 mg/mL MTT reagent for 4 h in the dark and mixed with DMSO (200 μl/ well). Finally, a microplate reader was used to detect the absorbance of the 96-well plate at a wavelength of 492 nm. Blank wells were used as controls to calculate the effect of RSV on cell activity.

Animals and treatment

C57BL/6J ApoE$^{-/-}$ mice (Card Vince, Changzhou, China) were nine-week-old male. All animal experiments were performed in accordance with the Guidelines for The Care and Use of Experimental Animals of Yunnan Agricultural University and approved by the Animal Ethics Committee of Yunnan Agricultural University (YNAU2024LLWYH005-1). No adverse events were observed during the study period. In the experiment, all mice were randomly divided into 7 groups. The specific groups and feeding methods were as follows: Control group (LFD): fed standard diet ($n = 6$). High-fat group (HFD): fed a high-fat diet (40% fat, Jiangsu Synbio-Engineering Co., LTD., XT108C) ($n = 6$). Lovastatin group (LOV): fed a high-fat diet and administered Lovastatin (20 mg/kg/d) by gavage every day. Resveratrol low-dose group (RSV-10): fed a high-fat diet and administered RSV (concentration of 2 mg/mL, 10 mg/kg/d) by gavage every day ($n = 8$) [21, 24]. Resveratrol high-dose group (RSV-20): fed a high-fat diet and administered RSV (concentration of 4 mg/mL, 20 mg/kg/d) by gavage every day ($n = 8$) [21, 24]. Gefitinib group: fed a high-fat diet and administered Gefitinib (concentration of 1 mg/mL, 5 mg/kg/d) by gavage every day ($n = 8$). The combination group (Gefitinib + RSV-20): fed a high-fat diet and administered Gefitinib (5 mg/kg/d) and RSV (20 mg/kg/d) by gavage every day ($n = 8$). Gavage was administered once a day for 10 weeks. At the end of the experiment, mice were euthanized and their liver and arterial tissues were collected for subsequent analysis.

DiI-LDL uptake assay

After placing round coverslips into the 12-well plate, HepG2 cells were seeded into dishes and starved in serum-free medium for 4 h. Then, RSV (0–30 μM) were added to the medium and incubated with cells. Subsequently, DiI-LDL (10 μg/mL, 20614ES76, Yeasen, Shanghai, China) was added to plates and incubated for 4 h in the dark. Cells were fixed with 4% paraformaldehyde for 20 min after washing with PBS. After the round coverslips were removed, nuclei were stained by DAPI. LDL uptake was finally observed under a fluorescent microscope and the fluorescence intensity reflected efficiency of LDL uptake by cells.

RT-qPCR

HepG2 cells and liver tissue from ApoE$^{-/-}$ mice were lysed using TransZol Up reagent (ET111-01-V2, TransGen, Beijing, China). Subsequently, samples were added with chloroform, covered, shaken vigorously for 15 s and left for 10 min. After centrifugation at 4°C and 12,000 rpm for 15 min, the upper aqueous phase was removed after stratification. The same volume of isopropanol was added to the upper aqueous phase. Then, the two liquids were gently mixed, placed for 10–15 min and centrifuged at 12,000 rpm for 10 min. Finally, total RNA was obtained. Next, reverse transcription experiments were performed using the PrimeScript RT reagent kit (RR037B, Takara, Dalian, China). Firstly, RNA was dissolved in DEPC water. Concentration and purity of RNA were determined using a spectrophotometer. After that, RNA was reverse transcribed into cDNA. Then, the qPCR reaction system was configured, including cDNA template, primer and qPCR Mix (including SYBR Green, RR820Q, Takara, Dalian, China). The reaction system was added to a 384-well plate with 10 μL per well. The program was set on the qPCR instrument as follows: predenaturation at 95°C for 30 s, denaturation at 95°C for 5 s, annealing and extension at 60°C for 30 s by 40 cycles. After the reaction, the amplification curve and dissolution curve were analyzed. The expression of LDLR gene was calculated (using the 2-ΔΔCt method) and β-actin was used as a control. The primer sequences used in this experiment are listed in Table 1.

Western blot experiment

Cells and mouse liver tissues were lysed using RIPA lysis buffer supplemented with 1% PSMF (R0010, Solarbio, Beijing, China) and total protein was extracted. Protein concentration was quantified by BCA method (P0012,

Table 1 Sequences of primers for RT-qPCR

Gene	Forward primer	Reverse primer
Human LDLR	GAACCCATCAAAGAGTGCG	TCTTCCT-GACCTCGTGCC
Human β-actin	CCCTGGCACCCAGCAC	GCCGATCCA-CACGGAGTAC
Mouse LDLR	GTGCTGGATGGGGAGGTCT	GAGGAACTG-GCGGCTGAA
Mouse β-actin	GTGACGTTGACATCCGTAAAGA	GCCGGACT-CATCGTACTCC

Beyotime, Jiangsu, China). Protein samples were mixed with loading buffer and denatured by boiling. Subsequently, SDS-PAGE gel electrophoresis was performed. The gel concentration of 8% was selected according to the molecular weight of target protein. After the experiment, total protein was transferred from the gel to PVDF membrane. The membrane was then blocked with 5% BSA for 1 h to reduce non-specific binding. After that, primary antibodies (LDLR, EGFR, P-EGFR, ERK, P-ERK and β-actin) diluted to 1:1000 in antibody diluent were added and incubated overnight at 4ºC. Next day, the membranes were washed with Tris Buffered Saline containing Tween 20® (TBST) three times for 10 min each, followed by the addition of secondary antibodies (horseradish peroxidase labeled anti-mouse or anti-rabbit IgG, Youweining, Shanghai, China) and incubation for 1 h at room temperature. Finally, after washing the PVDF membrane three times with TBST, chemiluminescence reagent A and B were mixed proportionally and evenly applied onto the PVDF membrane for light-avoidance chromogenic detection. Subsequently, gel imaging and photography were performed using a gel imager followed by analysis of strip intensity using ImageJ software version 1.44.

LDLR mRNA stability experiment

HepG2 cells were seeded in 10 dishes at 600 mm. Then, actinomycin D (5 μg/mL, Merck, Damstatt, Germany) was added to all dishes. After that, all dishes were divided into two groups: control and drug treatment group. And five dishes of drug treatment group were added with RSV (20 μM). Subsequently, RNA was extracted at 0 h, 0.5 h, 1 h, 2 h and 3 h in each group. LDLR mRNA expression was detected by RT-qPCR. The decay curve was drawn according to time.

Oil red O staining

Mouse aorta, sections of aortic sinus and livers were collected and stained following the instructions provided in the modified Oil Red O kit. Initially, tissue samples were fixed in 4% paraformaldehyde for 5 min to preserve cellular morphology. Subsequently, they were immersed in 60% isopropanol for 40 s to remove excess water. Samples were then treated with Oil red O working solution for 15 min to ensure complete binding of the intracellular lipids by the Oil red O reagent. Following this step, samples underwent washing with 60% isopropanol and distilled water twice each. Finally, observation and analysis of these samples were conducted using a Leica DM2500 microscope (Wetzlar, Germany) with images captured accordingly.

Elastic Van Gieson staining (EVG staining)

The aortic sinus tissues of $ApoE^{-/-}$ mice was sectioned and placed in a Petri dish containing EVG dye in order to ensure complete exposure of each section to the dye. Subsequently, EVG dye penetrated the sections and selectively stained the elastic fibers in order to enhance their visibility under microscopic examination. Excess dye was removed by rinsing the immersed aortic sinus sections with tap water. During this rinsing process, careful attention was paid to controlling the flow rate and strength of water to prevent any damage to the sections. The rinsed aortic sinus sections were then observed under a microscope to evaluate background color and changes in elastic fiber staining pattern. Optimal imaging conditions were achieved by adjusting both focal length and brightness settings on the microscope.

Immunofluorescence staining

The aortic sinus tissues from $ApoE^{-/-}$ mice were sectioned and fixed with 4% neutral formaldehyde for 15 min at room temperature. Sections were then treated with 0.3% Triton X-100 for 10 min to increase permeability, blocked with BSA and placed in a wet box. Subsequently, the sections were incubated overnight at 4ºC with the CD68 antibody. Then, the sections were left at room temperature for 15 min before antibody removal and were subjected to another round of incubation with the secondary antibody for 1 h. After thorough washing with PBS, the sections were immersed in a DAPI dye solution to stain the nuclei blue, dropped with anti-fluorescence attenuation sealant and then sealed with a glass cover. Finally, the expression of CD68 and the staining of nuclei were observed under a fluorescence microscope.

Immunohistochemical staining

First, the sections were dewaxed and hydrated at room temperature, followed by thermal antigen retrieval, which was applied to the hydrated sections. The sections were then placed in a humidified chamber with an immunohistochemical pen forming a circle and a small amount of distilled water was added to maintain humidity. Subsequently, goat serum blocking solution was applied and incubated at room temperature for 10 min. After removing the blocking solution, an antibody was applied to the tissue section and returned to the humidified chamber overnight. In the morning, the chamber was taken out from 4ºC refrigerator and allowed to equilibrate at

room temperature for 30 min. DAB substrate was added for 2 min, followed by washing with tap water. Brucine staining (approximately 1–2 min) until nuclei turned blue indicated completion of reaction. Further washing with tap water or PBS ensued before sealing with neutral gum. Subsequently, images were captured using a microscope (Nikon Eclipse Ti-E, Tokyo, Japan).

Statistical analysis

Data were expressed as the mean ± standard error of the mean (SEM). All experiments were repeated three times. Protein bands were analyzed using Image J software. Image-Pro Plus 6.0 was used to analyze plaque area and other staining area. All data were analyzed using GraphPad Prism 8.0. "One-way ANOVA" was used to evaluate statistical differences within groups. A significance level of $P < 0.05$ was considered statistically significant.

Result

RSV enhanced DiI-LDL uptake in HepG2 cells by upregulating LDLR expression

Firstly, after incubation with RSV for 24 h, HepG2 cell viability was analyzed using MTT assay. The results demonstrated that RSV exhibited no cytotoxic effects on HepG2 cells within 10–30 μM range (Fig. 1A). Consequently, the concentrations of 10, 20 and 30 μM were

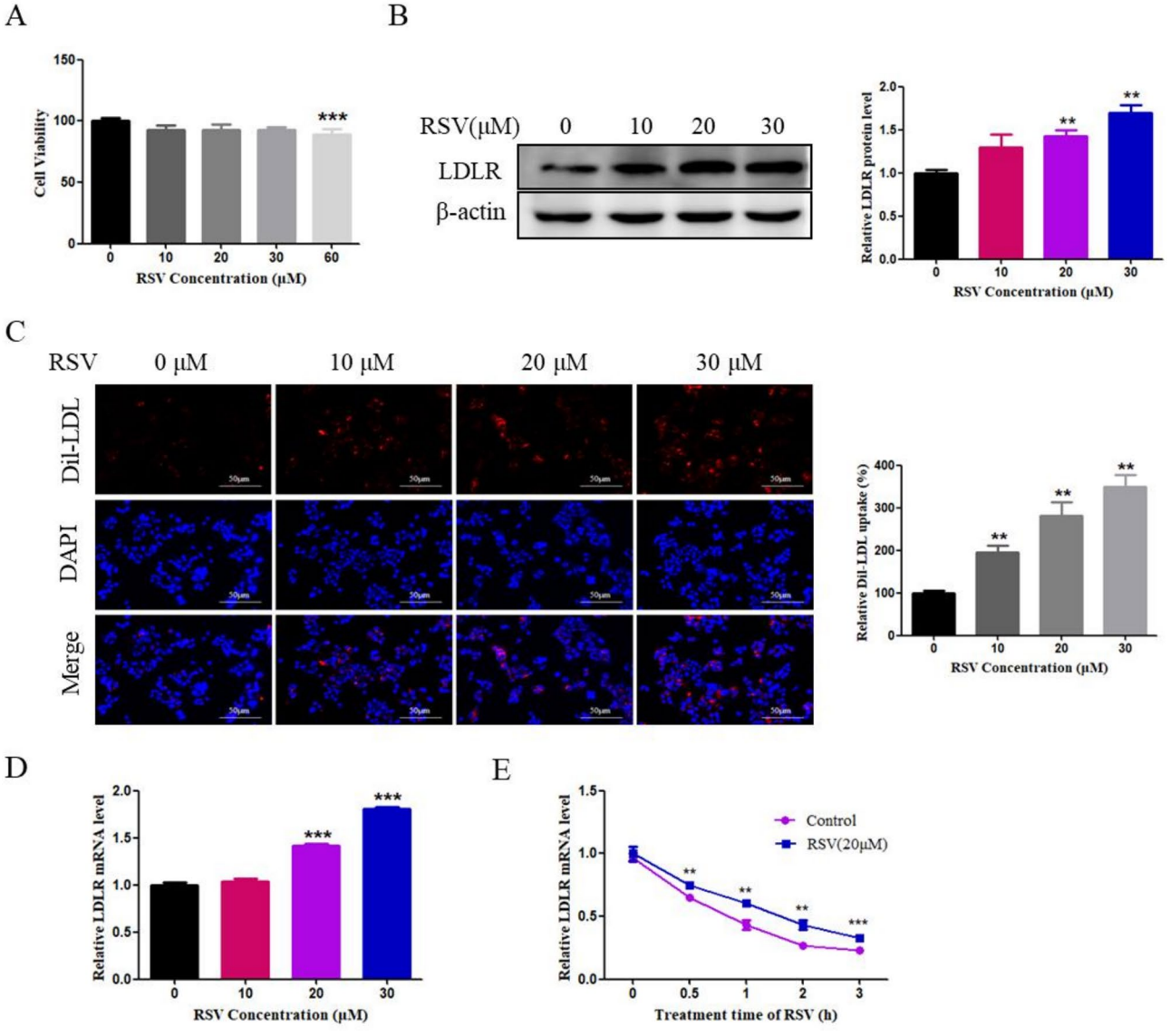

Fig. 1 RSV elevated DiI-LDL uptake by increasing LDLR expression. (**A**) After treated HepG2 cells with RSV (10, 20 and 30 μM), cell viability was measured by MTT assay. (**B**, **C**) Western blot and RT-PCR were performed to assess LDLR protein and mRNA levels, respectively. (**D**) DiI-LDL uptake was detected under a fluorescence microscope. (**E**) HepG2 cells were exposed to actinomycin D and RSV (20 μM), followed by RT-qPCR analysis to assess LDLR mRNA level. Date are expressed as mean ± SEM. Significant differences versus the control group are denoted by $^{**}P < 0.01$ and $^{***}P < 0.001$

selected for subsequent experiments. Around 70% of LDL-C circulation is removed through LDLR-dependent endocytosis. In order to explore how RSV affects LDLR expression, western blot was performed to examine RSV-induced changes in LDLR protein expression. Notably, experimental results indicated that RSV significantly enhanced LDLR protein expression (Fig. 1B). In circulation, low-density lipoprotein (LDL) serves as the primary cholesterol carrier. To examine the role of RSV on cholesterol metabolism, the effect of RSV on LDL uptake was evaluated through DiI-LDL assay. This assay measured fluorescence intensity to assess cellular LDL uptake capacity, which revealed a concentration-dependent promotion of LDL uptake by RSV (Fig. 1C). To further explore the mechanism of RSV promoting LDLR protein expression, RT-qPCR was performed to assess LDLR mRNA expression. The results showed that RSV promoted LDLR mRNA expression (Fig. 1D). Like transcription and translation, mRNA half-life is also strictly regulated and is an important factor affecting protein expression. To further elucidate the regulatory mechanism of RSV on LDLR gene expression, its impact on LDLR mRNA stability was investigated using actinomycin D blocking DNA transcription. The result showed that the degradation rate of LDLR mRNA decreased and RSV enhanced LDLR stability (Fig. 1E). These findings indicated that RSV could increase HepG2 cells' LDL uptake capacity through stabilizing LDLR mRNA and thereby increasing LDLR protein level.

RSV activated EGFR-ERK1/2 signaling pathway to promote LDLR expression in HepG2 cells

The above studies found that RSV reduced the degradation rate of LDLR mRNA. These findings provided valuable insights for future investigations into the molecular mechanisms underlying RSV-mediated regulation of LDLR expression. Previous studies have reported that activation of EGFR-ERK could stabilize LDLR mRNA [11]. This suggests a potential role for RSV in modulating LDLR mRNA stability through its influence on EGFR-ERK. To validate this hypothesis, more experiments were conducted. Western blot revealed that increasing concentrations of RSV corresponded to elevated P-EGFR and P-ERK1/2 protein levels (Fig. 2A). It indicated that RSV may stabilize LDLR mRNA through activating EGFR-ERK signaling pathway. To further corroborate these findings, Cetuximab (an EGFR monoclonal antibody) was employed to inhibit EGFR signaling in HepG2 cells. A significant attenuation in both EGFR and ERK1/2 activation induced by RSV was observed as well as the decrease in LDLR protein expression and impaired functionality related to LDL uptake ability (Fig. 2B, C). In summary, all these results demonstrated that RSV enhanced intracellular level of LDLR by stabilizing its mRNA stability via modulation of EGFR-ERK1/2 signaling pathway. Thereby it increased the capacity of HepG2 cells for efficient uptake of LDL.

RSV ameliorated atherosclerosis in ApoE$^{-/-}$ mice fed a high-fat diet

Given that the pathological characteristics and progression of AS in ApoE$^{-/-}$ mice closely mirror those observed in humans, C57BL/6J ApoE$^{-/-}$ mice were employed to evaluate the effects of RSV on LDLR expression and ameliorate AS. To assess therapeutic effect of RSV on AS, the mice were assigned to seven groups: LFD group, HFD group, LOV group, RSV-10 group, RSV-20 group, Gefitinib group and Gefitinib + RSV group. This grouping design allowed for a comprehensive study of the mechanisms and effects of RSV on AS. Plaque formation is a crucial indicator in atherosclerosis pathology [20]. Oil Red O staining was performed to evaluate the development of lesions in ApoE$^{-/-}$ mice. The results exhibited a significant increase in both aortic and aortic root plaque area in HFD group compared to LFD group. However, plaque deposits in LOV group were significantly reduced compared to HFD group. These findings confirmed the successful establishment of atherosclerosis model and indicated that the experimental conditions remained stable throughout the study. Simultaneously, the study found that the plaque area of RSV-10 and RSV-20 groups was also significantly reduced compared to HFD group. It indicated that RSV had a significant improvement effect on AS. Gefitinib group and Gefitinib + RSV group had no effect on reducing plaque deposits of aorta and aortic root of ApoE$^{-/-}$ mice (Fig. 3A, B).

Additionally, HFD group showed significantly increase of lipid-rich area in aortic root compared to LFD group. However, treatment with LOV, RSV-10 and RSV-20 groups resulted in a significant reduction in lipid-rich core area of the aortic root. Conversely, neither Gefitinib alone nor combined with RSV treatment had any effect on reducing the lipid-rich core area of aortic root (Fig. 4A). The infiltration of inflammatory cells in aortic root was further analyzed using the CD68 immunofluorescence staining method. The results demonstrated the significant increase in CD68 accumulation in aortic root of ApoE$^{-/-}$ mice fed with a high-fat diet compared to LFD group. However, treatment with LOV, RSV-10 and RSV-20 resulted in reduced CD68 accumulation. Gefitinib alone or combined with RSV did not affect it (Fig. 4B). Additionally, EVG staining was used to analyze the changes in elastic fibers in the aortic root. The findings revealed the extremely significant decrease in elastic fiber count of HFD group compared to LFD group. However, treatment with LOV, RSV-10 and RSV-20 resulted in a higher count of elastic fibers. Gefitinib alone or combined with RSV did not influence it (Fig. 4C). These

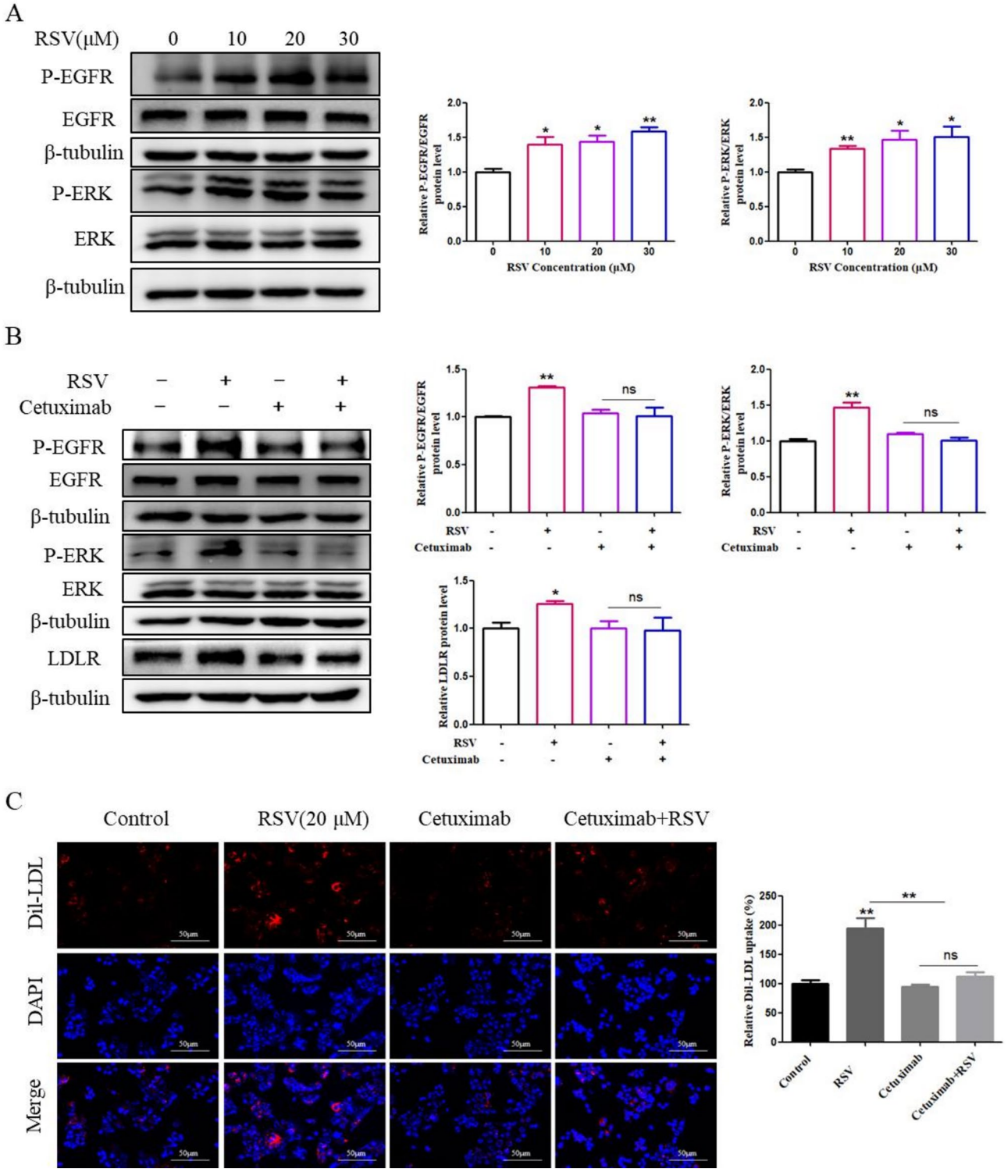

Fig. 2 RSV activated EGFR-ERK1/2 signaling pathway to promote LDLR expression. (**A**) HepG2 cells were exploed to RSV (10 μM, 20 μM and 30 μM). Expression levels of P-EGFR, EGFR, ERK and P-ERK were analyzed by western blot. (**B**) Cetuximab (5 μg/ml) and RSV (20 μM) were co-administered to HepG2 cells. Protein levels of P-EGFR, EGFR, ERK, and P-ERK were assessed using western blot analysis. (**C**) Dil-LDL uptake was visualized under a fluorescence microscope. Date are expressed as mean ± SEM. Significant differences versus the control group are denoted by $^{*}P < 0.05$, $^{**}P < 0.01$, $^{***}P < 0.001$

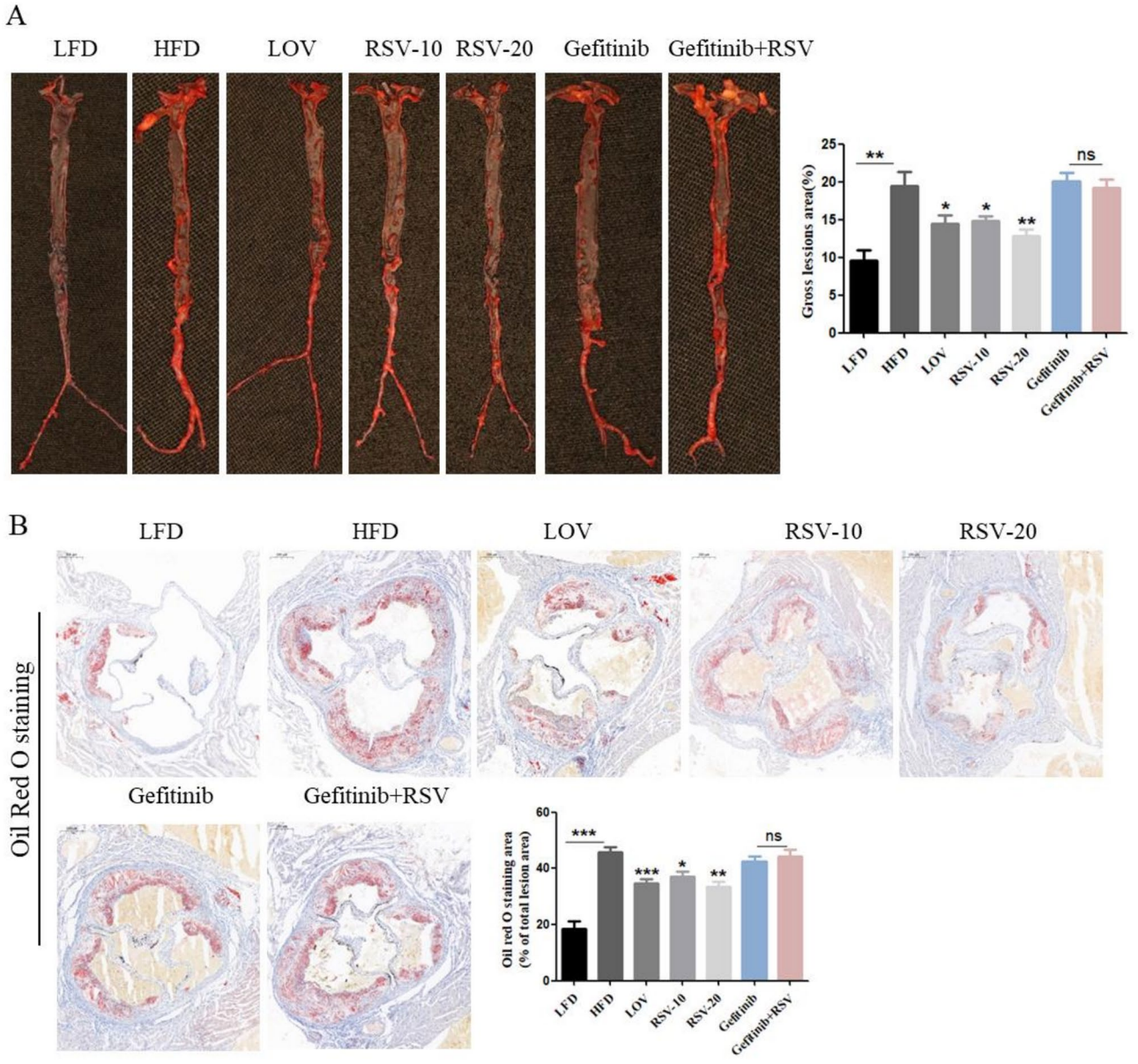

Fig. 3 RSV reduced aortic plaque formation in high-fat diet-fed ApoE$^{-/-}$ mice. (**A**, **B**) The presence of plaques in the aorta and aortic sinuses was assessed through Oil red O staining and the area of these plaques was quantified using Image J. Date are expressed as mean ± SEM. Significant differences versus the control group are denoted by $^{*}P < 0.05$, $^{**}P < 0.01$ and $^{***}P < 0.001$ ($n = 6$)

findings collectively indicated that RSV can ameliorate the onset and progression of AS.

RSV promoted LDLR expression in HFD-fed ApoE$^{-/-}$ mice by activating EGFR/ERK signaling pathway

In *vitro*, studies showed that RSV significantly increased LDLR gene expression by activating EGFR-ERK1/2 signaling pathway. To determine whether biological effects of RSV in *vivo* is consistent with the results in *vitro*, RT-qPCR was employed to assess the impact of RSV on LDLR mRNA in mouse livers. The date showed that LDLR mRNA levels of RSV-10 and RSV-20 were increased compared to HFD group. However, there was no notable change observed in LDLR mRNA levels among ApoE$^{-/-}$ mice receiving Gefitinib group or Gefitinib + RSV group (Fig. 5A). Subsequently, western blot and immunohistochemistry technique were utilized to confirm the effect of RSV on related protein levels (LDLR, P-EGFR and P-ERK) within liver tissues. Compared to HFD group, ApoE$^{-/-}$ mice administered RSV (10 and 20 mg/kg/d) exhibited significantly higher levels of LDLR, P-EGFR and P-ERK protein. The results were consistent with cell-based experiments. However, no substantial differences were observed for these proteins

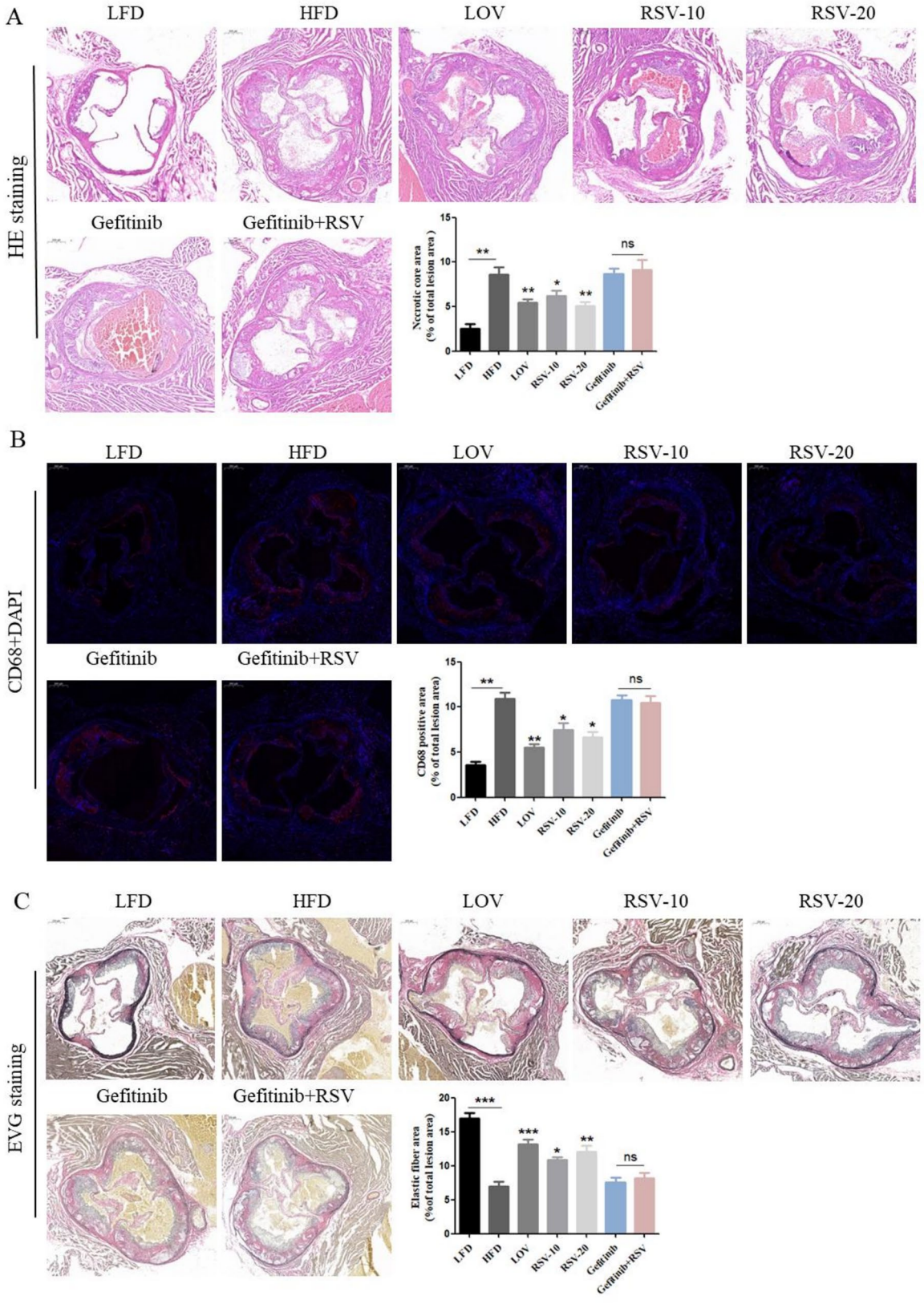

Fig. 4 RSV enhanced plaque stability in a high-fat diet ApoE$^{-/-}$ mice. (**A**, **C**) H&E and EVG staining were performed on aortic sinus sections to assess the necrotic core area and elastic fiber content, respectively. (**B**) Immunofluorescent staining was performed on aortic sinus section to assess macrophage deposition. Date are expressed as mean ± SEM. Significant differences versus the control group are denoted by *$P < 0.05$, **$P < 0.01$ and ***$P < 0.001$ ($n = 6$)

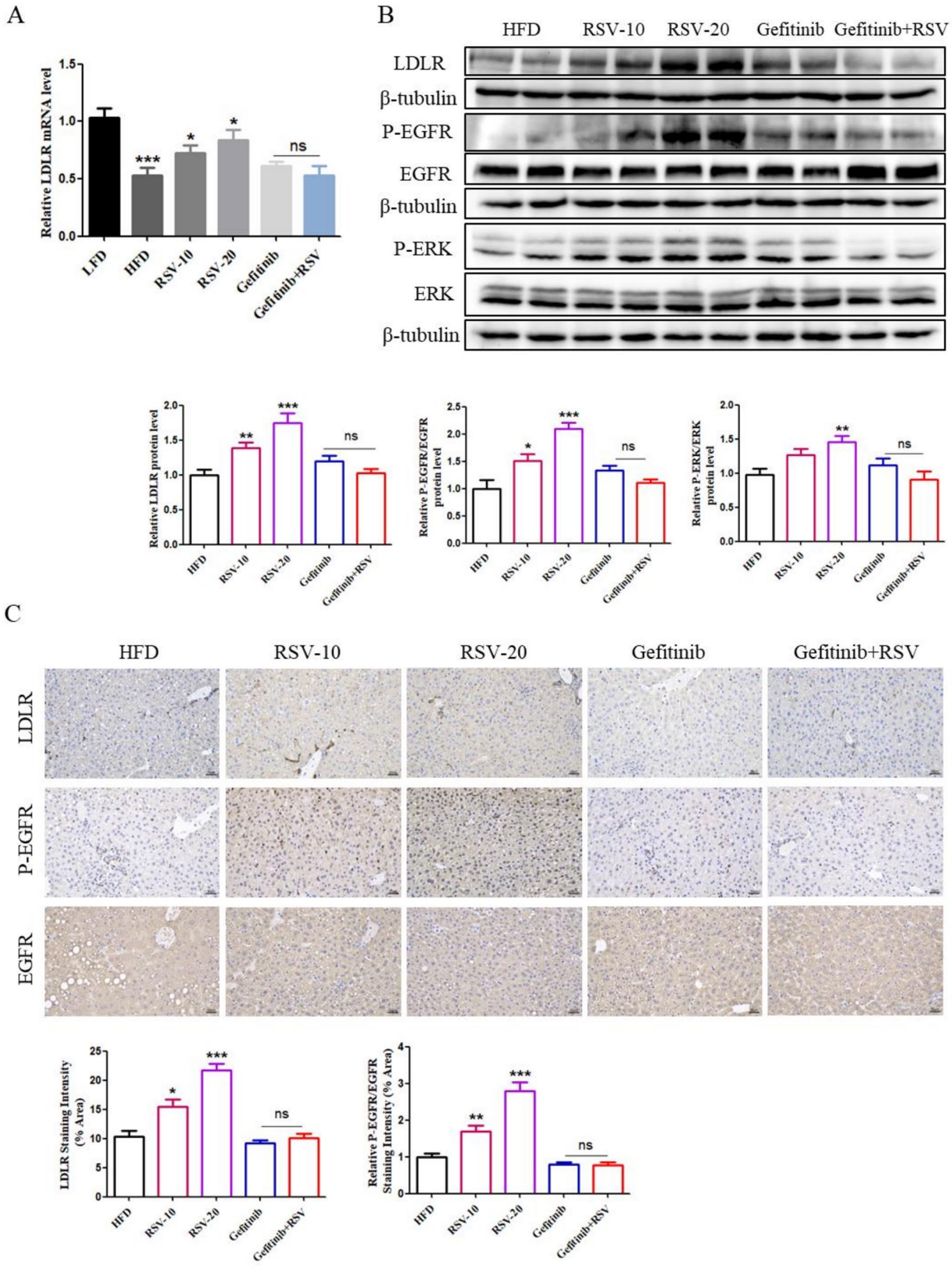

Fig. 5 RSV enhanced LDLR expression by activating EGFR-ERK signaling pathway in high-fat diet-fed ApoE$^{-/-}$ mice. (**A**) The mRNA expression of LDLR in livers was measured by RT-qPCR. (**B**) Western blot was performed to measure protein levels of LDLR, P-EGFR, EGFR, P-ERK and ERK in lives. (**C**) Immunohistochemical staining was used to analyze LDLR, P-EGFR and EGFR expression in livers. Date are expressed as mean ± SEM. Significant differences versus the control group are denoted by *$P < 0.05$, **$P < 0.01$ and ***$P < 0.001$ ($n = 6$)

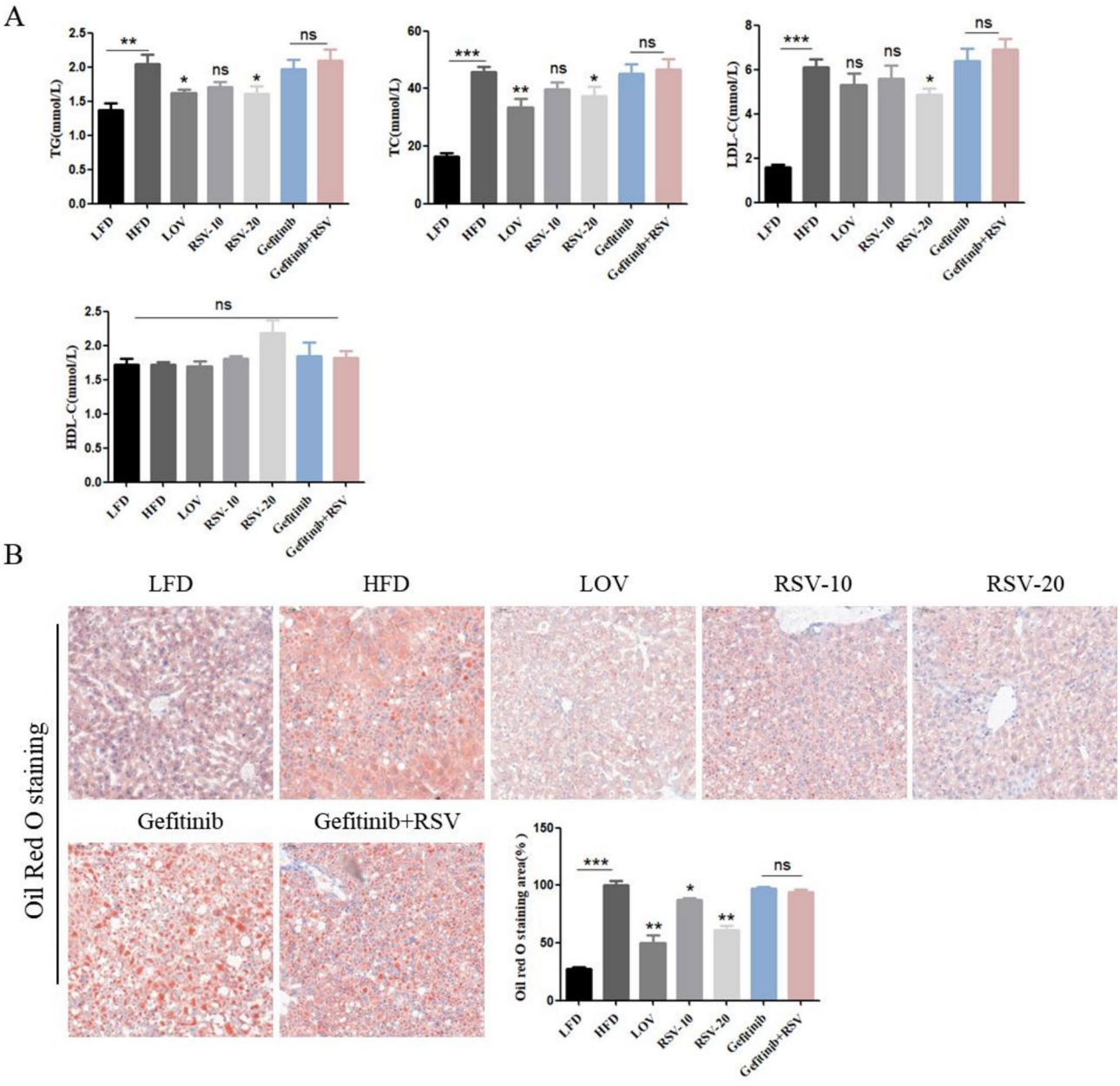

Fig. 6 RSV reduced liver lipid accumulation and improved blood lipid biochemical indices. (**A**) Serum levels of TG, TC, LDL-C and HDL-C were measured in ApoE$^{-/-}$ mice. (**B**) Oil red O staining was employed to detect lipid deposition in livers. Date are expressed as mean ± SEM. Significant differences versus the control group are denoted by $^{*}P < 0.05$, $^{**}P < 0.01$ and $^{***}P < 0.001$ ($n = 6$)

between ApoE$^{-/-}$ mice receiving Gefitinib group or Gefitinib + RSV group (Fig. 5B, C). Collectively, these findings suggested that activating EGFR-ERK1/2 by RSV may enhance hepatic expression of LDLR.

RSV reduced liver lipid accumulation and improved blood lipid biochemical indices

Dysregulated lipid metabolism is a key factor in the pathogenesis of AS. To further substantiate that RSV improved AS by enhancing LDL clearance, serum lipid profiles were examined in ApoE$^{-/-}$ mice. The results demonstrated that TG and TC levels in ApoE$^{-/-}$ mice treated with LOV and RSV-20 were significantly reduced. Notably, LDL-C level was also markedly reduced in RSV-20 group. Although LDL-C level in LOV group exhibited a trend toward reducing, this effect was not statistically significant. Meanwhile, neither LOV nor RSV affected serum HDL-C levels. Neither Gefitinib alone nor in combination with RSV altered the serum lipid profiles (Fig. 6A). In addition, excessive fat intake can lead to hepatic lipid accumulation in the form of lipid droplets. Therefore, livers in HFD group exhibited substantially

higher lipid accumulation than those in LFD group, as evidenced by Oil Red O staining. However, this condition improved significantly in ApoE$^{-/-}$ mice treated with LOV, RSV-10 and RSV-20. In contrast, Gefitinib alone or in combination with RSV did not influence hepatic lipid accumulation (Fig. 6B). These findings further supported the hypothesis that RSV promoted LDLR expression, enhanced LDL clearance, improved lipid metabolism and reduced hepatic fat accumulation.

Discussion

As a global primary chronic disease, AS has become a significant challenge in the field of public health due to its high incidence and high mortality [25]. The core pathological feature of this disease is chronic inflammatory lesions caused by abnormal deposition of cholesterol in the arterial intima [26]. Substantial evidence confirmed that elevated plasma LDL-C level directly contribute AS pathogenesis as an independent risk factor [27]. Given that LDL is the principal vehicle for cholesterol transport in circulation, regulating its metabolism is a key focus in combating AS [28]. LDLR plays a pivotal role in cholesterol homeostasis by regulating plasma cholesterol level and is a critical component of cholesterol metabolic pathways [29]. This study revealed that RSV can ameliorate AS by activating EGFR-ERK signaling pathway and upregulating LDLR expression.

In HepG2 cells, RSV upregulated LDLR protein level through increasing post-transcriptional stabilization of LDLR mRNA and improved LDL uptake. However, at a concentration of 10 μM, this increase was not statistically significant. This may be attributed to the involvement of other intracellular receptors involved in lipoprotein metabolism such as scavenger receptors or alternative signaling pathways that indirectly influence LDL uptake efficiency through synergistic or compensatory mechanisms. Given that ANGPTL3 has been recognized as a key controller of lipoprotein metabolism [30, 31], RSV may also reduce circulating LDL-C levels by inhibiting ANGPTL3 to promote VLDL clearance. Therefore, it was hypothesized that the mechanism of action of RSV was not confined to the LDLR pathway alone but likely involves a complex multi-signal regulatory network.

Previous studies have demonstrated that ERK kinase can regulate gene expression by stabilizing the promoter region of LDLR. At the same time, this study found that RSV could significantly increase the phosphorylation levels of EGFR and ERK, which further verified the molecular mechanism of RSV regulation of LDLR expression. In addition, alterations in cholesterol metabolism are closely associated with EGFR signaling in certain aggressive cancers. EGFR mutations can enhance cellular cholesterol uptake by stimulating LDLR expression [32, 33]. Therefore, it may be an effective mechanism that RSV regulated LDL metabolism by activating EGFR-ERK signaling pathway.

In the high-fat diet-induced AS model of ApoE$^{-/-}$ mice, RSV was observed to significantly reduce arterial plaque deposition and the infiltration of macrophages. Meanwhile it increased content elastic fiber. Moreover, RSV improved lipid metabolism and reduced lipid accumulation in livers. These findings indicated that RSV exerted a substantial ameliorative effect on AS at appropriate doses. However, when RSV was combined with the EGFR inhibitor Gefitinib, the beneficial effects on plaque reduction were abrogated. This likely occurred because Gefitinib blocked EGFR signaling pathway, thereby counteracting the therapeutic effects of RSV. These results suggested a potential antagonistic interaction between RSV and Gefitinib.

Strengths and limitations

This study was the first to reveal the molecular mechanism by which RSV upregulates LDLR expression by activating EGFR-ERK signaling pathway. It provided novel ideas for targeted intervention. In addition, traditional studies have mainly focused on the antioxidant effect of RSV [34]. However, this study revealed a non-classical pathway through which RSV regulated lipid metabolism via EGFR and expanded the understanding of RSV pleiotropy.

Despite the achievements of this study, there are still some limitations that are not fully elucidated. First of all, RSV can significantly change the capacity of LDL uptake and LDLR expression level at a concentration of 10 μM in HepG2 cells, but the specific molecular mechanism of the regulation has not been fully understood. In addition, studies have shown that impaired ANGPTL3 function leads to a notable reduction in LDL-C, triglyceride-rich lipoproteins and concurrent risk reduction in development of coronary artery disease [35–37]. As a key regulator of lipid metabolism, ANGPTL3 is independent of the classical LDLR pathway, so it is a valuable research direction to explore whether RSV affects cholesterol metabolism by regulating ANGPTL3. Finally, the mechanism of interaction between RSV and cell membrane components needs to be elucidated including its regulation of membrane fluidity, membrane protein conformation and other physical properties. These breakthroughs in basic research not only help to reveal the multi-target characteristics of RSV, but also provide new theoretical basis and therapeutic targets for the intervention strategy of AS. Moreover, to achieve clinical translation of RSV, it is still necessary to systematically analyze its molecular network and comprehensively evaluate its regulatory efficacy on lipid metabolism.

Conclusion

In summary, this study revealed a novel mechanism of RSV upregulating LDLR expression by activating the EGFR-ERK1/2 signaling pathway and elucidated the molecular basis of its improvement in the occurrence and development of AS. This finding improves the understanding of mechanisms underlying the cardiovascular protective effects of RSV. At the same time, it provides a novel theoretical basis and potential therapeutic strategy for the targeted therapy of atherosclerotic cardiovascular diseases.

Supplementary Information

The online version contains supplementary material available at https://doi.org/10.1186/s12944-025-02585-8.

Supplementary Material 1

Acknowledgements
The data are available from the corresponding author upon reasonable request.

Author contributions
Jun Sheng, Xuan-Jun Wang and Ye-Wei Huang designed this research and revised the manuscript. Dan-Dan Hu, Lin Qi and Li-Tian Wang performed the investigation, formal analysis, visualization, project administration and writing-original draft. Dan-Dan Hu, Ya-Min Jin, Xiang-Xuan Yang, Huai-Liu Yin and Qi-xing Zhou performed the investigation, data curation and validation.

Funding
This study was supported by Yunnan Science and Technology Talents support plan (YNWR-QNBJ-2018-083) and Basic Research Program of Yunnan Province (202301BD070001-029).

Data availability
No datasets were generated or analysed during the current study.

Declarations

Ethical approval
All animal experiments were approved by the Animal Ethics Committee of Yunnan Agricultural University (YNAU2024LLWYH005-1).

Competing interests
The authors declare no competing interests.

Author details
[1]Key Laboratory of Pu-er Tea Science, Ministry of Education, Yunnan Agricultural University, Kunming 650201, China
[2]College of Science, Yunnan Agricultural University, Kunming 650201, China
[3]Faculty of Basic Medical Science, Kunming Medical University, Kunming 650500, China
[4]College of Food Science and Technology, Yunnan Agricultural University, Kunming 650201, China
[5]College of Resources, Environment, and Chemistry, Chuxiong Normal University, Chuxiong 675099, China

Received: 15 October 2024 / Accepted: 26 April 2025
Published online: 08 May 2025

References

1. Fan J, Watanabe T. Atherosclerosis: known and unknown. Pathol Int. 2022;72(3):151–60.
2. Zhang S, Picard MH, Vasile E, Zhu Y, Raffai RL, Weisgraber KH, Krieger M. Diet-induced occlusive coronary atherosclerosis, myocardial infarction, cardiac dysfunction, and premature death in scavenger receptor class B type I-deficient, hypomorphic Apolipoprotein ER61 mice. Circulation. 2005;111(25):3457–64.
3. Tietge UJ. Hyperlipidemia and cardiovascular disease: inflammation, dyslipidemia, and atherosclerosis. Curr Opin Lipidol. 2014;25:94–5.
4. Khatana C, Saini NK, Chakrabarti S, Saini V, Sharma A, Saini RV, Saini AK. Mechanistic insights into the oxidized Low-Density Lipoprotein-Induced atherosclerosis. Oxid Med Cell Longev. 2020;2020:5245308.
5. Matsumoto T, Takashima H, Ohira N, Tarutani Y, Yasuda Y, Yamane T, Matsuo S, Horie M. Plasma level of oxidized low-density lipoprotein is an independent determinant of coronary macrovasomotor and microvasomotor responses induced by Bradykinin. J Am Coll Cardiol. 2004;44(2):451–7.
6. Lagace TA, Curtis DE, Garuti R, McNutt MC, Park S, Prather HB. Secreted PCSK9 decreases the number of LDL receptors in hepatocytes and in livers of parabiotic mice. J Clin Invest. 2006;116(11):2995–3005.
7. Qian YW, Schmidt RJ, Zhang Y, Chu S, Lin A, Wang H, Wang X, Beyer TP, Bensch WR, Li W, Ehsani ME, Lu D, Konrad RJ, Eacho PI, Moller DE, Karathanasis SK, Cao G. Secreted PCSK9 downregulates low density lipoprotein receptor through receptor-mediated endocytosis. J Lipid Res. 2007;48(7):1488–98.
8. Canepari C, Milani M, Starinieri F, Fabiano A, Russo F, Norata R, Rocchi M, Biffi M, Sanvito F, Cantore A. Low-density lipoproteins receptor (LDLR) liver gene therapy normalizes LDL cholesterol (LDL-C) and prevents atherosclerosis in a Familial hypercholesterolemia (FH) mouse model. Atherosclerosis. 2024;395.
9. Wilson GM, Roberts EA, Deeley RG. Modulation of LDL receptor mRNA stability by phorbol esters in human liver cell culture models. J Lipid Res. 1997;38:437–46.
10. Wilson GM, Vasa MZ, Deeley RG. Stabilization and cytoskeletal-association of LDL receptor mRNA are mediated by distinct domains in its 3' untranslated region. J Lipid Res. 1998;39:1025–32.
11. Mnasri N, Mamarbachi M, Allen BG, Mayer G. 5-Azacytidine engages an IRE1α-EGFR-ERK1/2 signaling pathway that stabilizes the LDL receptor mRNA. Biochim Biophys Acta Gene Regul Mech. 2018;1861:29–40.
12. Bjune K, Wierød L, Naderi S. Triciribine increases LDLR expression and LDL uptake through stabilization of LDLR mRNA. Sci Rep. 2018;8:16174.
13. Huang YW, Wang LT, Zhang M, Nie Y, Yang JB, Meng WL, Wang XJ, Sheng J. Caffeine can alleviate non-alcoholic fatty liver disease by augmenting LDLR expression via targeting EGFR. Food Funct. 2023;14:3269–78.
14. Zhang LX, Li CX, Kakar MU, Khan MS, Wu PF, Amir RM, Dai DF, Naveed M, Li QY, Saeed M, Shen JQ, Rajput SA, Li JH. Resveratrol (RV): A Pharmacological review and call for further research. Biomed Pharmacother. 2021;143:112164.
15. Meng X, Zhou J, Zhao CN, Gan RY, Li HB. Health benefits and molecular mechanisms of Resveratrol: A narrative review. Foods. 2020;9.
16. Lu KT, Ko MC, Chen BY, Huang JC, Hsieh CW, Lee MC, Chiou RY, Wung BS, Peng CH, Yang YL. Neuroprotective effects of Resveratrol on MPTP-induced neuron loss mediated by free radical scavenging. J Agric Food Chem. 2008;56(16):6910–3.
17. Csiszar A. Anti-inflammatory effects of Resveratrol: possible role in prevention of age-related cardiovascular disease. Ann N Y Acad Sci. 2011;1215:117–22.
18. Reçica R, Kryeziu I, Thaçi Q, Avtanski D, Mladenov M, Basholli-Salihu M, Sopi RB. Protective effects of Resveratrol against airway hyperreactivity, oxidative stress, and lung inflammation in a rat pup model of bronchopulmonary dysplasia. Physiol Res. 2024;73(2):239–51.
19. Jing Y, Hu T, Yuan J, Liu Z, Tao M, Ou M, Cheng X, Cheng W, Yi Y, Xiong Q. Resveratrol protects against postmenopausal atherosclerosis progression through reducing PCSK9 expression via the regulation of the ERα-mediated signaling pathway. Biochem Pharmacol. 2023;211:115541.
20. Chen ML, Yi L, Zhang Y, Zhou X, Ran L, Yang J, Zhu JD, Zhang QY, Mi MT. Resveratrol attenuates Trimethylamine-N-Oxide (TMAO)-Induced atherosclerosis by regulating TMAO synthesis and bile acid metabolism via remodeling of the gut microbiota. mBio. 2016;7(2):e02210–15.
21. Ye G, Chen G, Gao H, Lin Y, Liao X, Zhang H, Liu X, Chi Y, Huang Q, Zhu H, Fan Y, Dong S. Resveratrol inhibits lipid accumulation in the intestine of atherosclerotic mice and macrophages. J Cell Mol Med. 2019;23(6):4313–25.
22. Akbari M, Tamtaji OR, Lankarani KB, Tabrizi R, Dadgostar E, Haghighat N, Kolahdooz F, Ghaderi A, Mansournia MA, Asemi Z. The effects of Resveratrol on lipid profiles and liver enzymes in patients with metabolic syndrome

and related disorders: a systematic review and meta-analysis of randomized controlled trials. Lipids Health Dis. 2020;19:25.
23. Chen J, Liu Y, Liu Y, Peng J. Resveratrol protects against ox-LDL-induced endothelial dysfunction in atherosclerosis via depending on circ_0091822/miR-106b-5p-mediated upregulation of TLR4. Immunopharmacol Immunotoxicol. 2022;44:915–24.
24. Guo S, Zhou Y, Xie X. Resveratrol inhibiting TGF/ERK signaling pathway can improve atherosclerosis: backgrounds, mechanisms and effects. Biomed Pharmacother. 2022;155:113775.
25. Mozaffarian D, Benjamin EJ, Go AS, Arnett DK, Blaha MJ, Cushman M, de Ferranti S, Després JP, Fullerton HJ, Howard VJ, et al. Heart disease and stroke statistics–2015 update: a report from the American heart association. Circulation. 2015;131:e29–322.
26. Meens MJ, Pfenniger A, Kwak BR. Risky communication in atherosclerosis and thrombus formation. Swiss Med Wkly. 2012;142:w13553.
27. Guijarro C, Cosín-Sales J. LDL cholesterol and atherosclerosis: the evidence. Clin Investig Arterioscler. 2021;33(Suppl 1):25–32.
28. Qiao YN, Zou YL, Guo SD. Low-density lipoprotein particles in atherosclerosis. Front Physiol. 2022;13:931931.
29. Bulbulia R, Armitage J. LDL cholesterol targets–how low to go? Curr Opin Lipidol. 2012;23:265–70.
30. Kersten S. ANGPTL3 as therapeutic target. Curr Opin Lipidol. 2021;32(6):335–41.
31. Chen PY, Gao WY, Liou JW, Lin CY, Wu MJ, Yen JH. Angiopoietin-Like protein 3 (ANGPTL3) modulates lipoprotein metabolism and dyslipidemia. Int J Mol Sci. 2021;22(14):7310.
32. Fang R, Chen X, Zhang S, Shi H, Ye Y, Shi H, Zou Z, Li P, Guo Q, Ma L, He C, Huang S. EGFR/SRC/ERK-stabilized YTHDF2 promotes cholesterol dysregulation and invasive growth of glioblastoma. Nat Commun. 2021;12(1):177.
33. Luo Y, Yang Y, Peng P, Zhan J, Wang Z, Zhu Z, Zhang Z, Liu L, Fang W, Zhang L. Cholesterol synthesis disruption combined with a molecule-targeted drug is a promising metabolic therapy for EGFR mutant non-small cell lung cancer. Transl Lung Cancer Res. 2021;10:128–42.
34. Wang H, Yang YJ, Qian HY, Zhang Q, Xu H, Li JJ. Resveratrol in cardiovascular disease: what is known from current research? Heart Fail Rev. 2012;17(3):437–48.
35. Xu YX, Redon V, Yu H, Querbes W, Pirruccello J, Liebow A, Deik A, Trindade K, Wang X, Musunuru K, Clish CB, Cowan C, Fizgerald K, Rader D, Kathiresan S. Role of angiopoietin-like 3 (ANGPTL3) in regulating plasma level of low-density lipoprotein cholesterol. Atherosclerosis. 2018;268:196–206.
36. Tikka A, Jauhiainen M. The role of ANGPTL3 in controlling lipoprotein metabolism. Endocrine. 2016;52(2):187–93.
37. Luo F, Das A, Khetarpal SA, Fang Z, Zelniker TA, Rosenson RS, Qamar A. ANGPTL3 Inhibition, dyslipidemia, and cardiovascular diseases. Trends Cardiovasc Med. 2024;34(4):215–22.

Publisher's note